

## Corrosion Performance of Superhex Heater Tubes Exposed to Alumina Refinery Plant Conditions

Darwin Del Aguila<sup>1</sup> and Joseph Del Aguila<sup>2</sup>

1. Corrosion Scientist

2. Director

Aushex Pty Ltd, Director, Brisbane, Australia

Corresponding author: d.delaguila@aushex.com

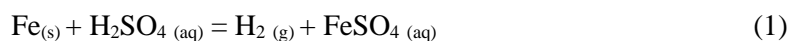
### Abstract

Superhex is a high acid corrosion resistance heat exchanger tube that has been exposed to the alumina refinery process condition for the first time in January 2021. Two brand-new heat exchanger units have been tubed with this material and its corrosion performance monitored during the acid wash and Bayer liquor exposure. Its corrosion performance was monitored using a corrosion probe positioned between two live steam heaters (LSH) of an evaporation train and the corrosion rate in millimeters/year (mmpy) was measured from electrochemistry data of linear polarization resistance (LPR) and impedance. Unlike the corrosion assessment in the laboratory; where the parameters surrounding the corrosion cell are controlled and consequently clear electrochemistry data is obtained, the data obtained in the plant is affected by the presence of corrosion inhibitor (low corrosion rates), scale formed during liquor flow (inaccurate corrosion data before the scale is dissolved), and pump mechanical condition (noisy data). It was also observed, that the exposure time of the tube during the acid wash is considerable shorter than during Bayer liquor exposure. Overall, Superhex showed better corrosion performance than the other materials under evaluation. One of the units containing the Superhex tubes will be opened for visual inspection around February 2022.

**Keywords:** Sulphuric acid, Corrosion resistance, ASTM 179, Heat exchanger tube.

### 1. Introduction

In its dilute form, sulphuric acid reacts with metals (e.g. iron) through Equation (1) producing hydrogen (gas) and metal sulfate (salt) on the metal surface [1, 2, 3] given by Equation (1):



Recent advanced technology on crystallography and passivation film [10] has identified key metallurgical parameters that can provide high corrosion resistance in acid solutions. Figure 1 shows an example of the in-laboratory behaviors of two cold-drawn low-carbon steel ASTM-179 tubes, with preferred versus unpreferred crystal grain orientation condition, after 15 h exposure to 6 % v/v **uninhibited** sulphuric acid at 60 °C and flow rate of 1 m/s. Significant corrosion of the unpreferred orientation (STD ASTM 179) with 94.3 wt. % mass loss in comparison to the relatively unaffected preferred orientation (Superhex) with only 5.5 wt. % mass loss. As previously presented (ICSOBA 2020), the main difference between Superhex and other low carbon steel HEX materials is the formation of a passive film in contact with dilute sulphuric [7] and hydrochloric acid that inhibits the corrosion attack by keeping at lower levels. The same materials tested in the laboratory were assembled in a corrosion probe and inserted into the Bayer process, between two live steam heaters of an evaporation train.



**Figure 1. Laboratory mass loss images of Superhex vs STD ASTM 179**

About 1000 tubes (lengths) of the Superhex material have been placed in each brand-new heat exchanger (HEX) unit and exposed to the alumina refinery process conditions as showed in Figure 2.



**Figure 2. HEX unit tubed with Superhex**

## **2. Experimental**

### **2.1 Sequency of Plant Operations**

This is the list of process operations before acid cleaning.

- Drain Bayer liquor from the system.
- Water flush to remove residual liquor and line up valves and pumps to the acid circuit.
- Pump acid and recirculation.

### **2.2 Description of Electrochemistry Instrumentation**

The corrosion setup used comprises a high-resolution potentiostat, multiplexer, data logger, laptop, and corrosion probe as shown in Figure 3.

The potentiostat supplies the electronic signals for the corrosion cell. The multiplexer allows to switch measurements from specimen to specimen and repeat them in a loop system. The data logger records the temperature across the whole process. The laptop drives the corrosion software and consequently controls all the instrumentation, and the corrosion probe holds the specimen under evaluation and exposes them to the real corrosion environment. A single electrical cable connects the cabinet with the probe which is inserted in the process pipe as shown in Figure 4.



Figure 3. Instrument cabinet



Figure 4. Corrosion probe

### Corrosion Probe: RP5

The corrosion probe is a high-pressure device assembled in a 50NB, 600 LB, R/F flange with internal electrical connections to each electrode and a high-pressure spring torque system to keep the whole assembly completely sealed and pressure safe.

The sample holder, shown in Figure 5, has 5 positions (electrodes). The electrodes are isolated using gasket gylon resistant to acid and caustic solution. P1, P2, and P4 positions for testing, and the material are all low carbon steel within the standard specification for seamless cold-drawn low-carbon steel heat exchanger and condenser tubes. The P3 and P5 positions for the reference and the counter electrode respectively to complete the electric circuit of the corrosion cell. Both are high nickel and copper materials (monel 400) suitable for this application.

For this particular test, the positions description are as follows:

- P1 is occupied by a piece of tube corresponding to a material specified for alumina refineries.
- P2 is occupied by a piece of tube corresponding to the STD ASTM 179 (all purposes material).
- P4 is occupied by a piece of tube corresponding to the Superhex.



Figure 5. Sample holder

### 2.3 Description of Electrochemistry Techniques

The above setup uses and measures corrosion using 3 corrosion techniques:

- Mass loss technique uses weight before and after exposure.
- LPR (Linear Polarization Resistance), uses direct current (DC) to measure the corrosion resistance of the material under evaluation.
- Impedance uses alternative current (AC) to measure the corrosion resistance of the material under evaluation. In this report, the author will use impedance data to highlight the corrosion resistance and LPR to calculate corrosion rate (CR).
- In impedance, the corrosion resistance ( $R_p$ ) is determined by the magnitude of the semicircle diameter of the Nyquist plot [8,9] as shown in Figure 6.

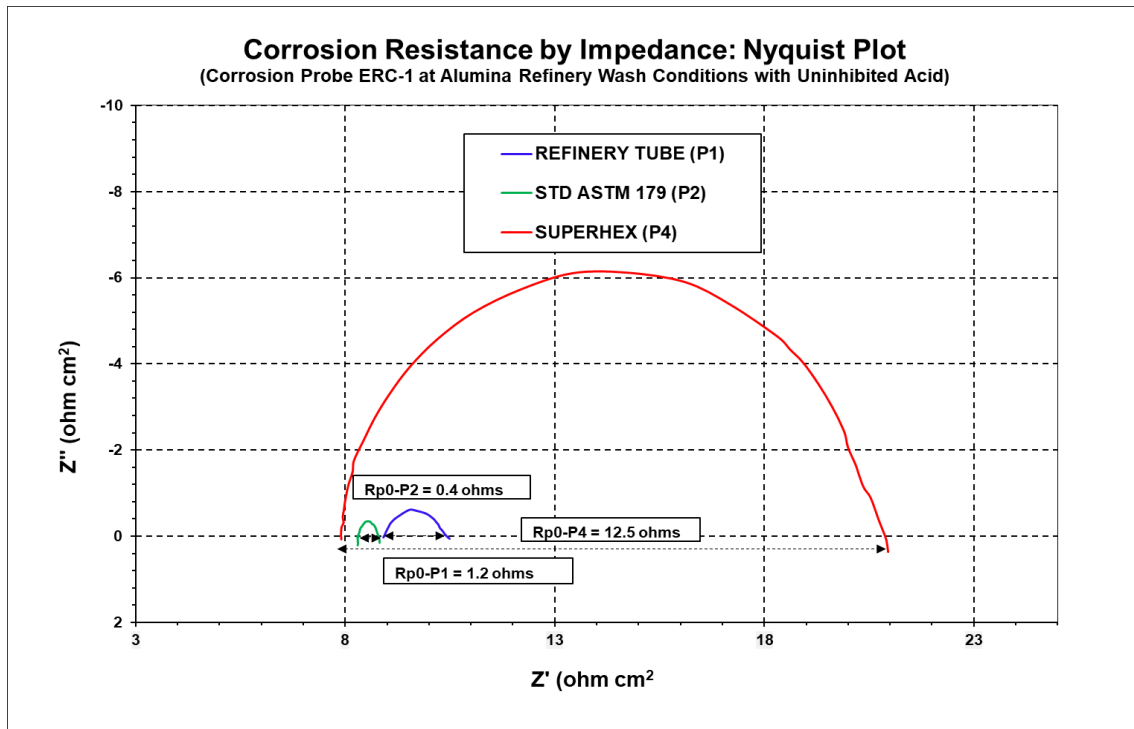


Figure 6. The Nyquist plot with uninhibited acid at washing conditions

- The corrosion program has been set up to sequentially measure open circuit potential (OCP), LPR, and impedance in each specimen under evaluation and is done in approximately 6 minutes consequently, the measurements on the 3 specimens are completed in about 18 minutes and then repeated in a loop.
- A run (loop) is defined as the consecutive measuring and completion of the 3 samples in the sample holder.
- Note: As long as the specimens are in the same corrosion environment and measured consecutively, the magnitude of their corrosion resistances are comparative and inversely proportional to their corrosion rates at that specific time: Higher corrosion resistance produces lower corrosion rate, consequently, less corrosion damage.

### 2.4 Calculation of Corrosion Rate [5]

Polarization resistance ( $R_p$ ), according to Faraday's law, is defined as the slope of potential vs current density given in Equation (2):

$$R_p = \frac{E}{i} \quad (2)$$

where:

$R_p$   
 $E$  Corrosion potential  
 $i$  Corrosion current

Corrosion current ( $i_{corr}$ ) is then calculated according to the Stern-Geary relationship given in Equation (3):

$$i_{corr} = \frac{\beta}{R_p} \quad (3)$$

where:

$\beta$  Stern-Geary coefficient determined as per Equation (4)  
 $R_p$  Corrosion resistance obtained from LPR or impedance,  $\Omega$   
 $i_{corr}$  Amp/cm<sup>2</sup>

$$\beta = \frac{\beta_a \times \beta_c}{2.3 \times (\beta_a + \beta_c)} \quad (4)$$

where:

$\beta_a$  Anodic Tafel Slope [4,6]  
 $\beta_c$  Cathodic Tafel Slope [4,6]  
 $\beta$  **0.115 Volts** (Experimentally determined) for Acid Solution  
 $\beta$  **0.001468 Volts** (Experimentally determined) for Bayer Liquor

From Faraday's Law:

$$m = \frac{E_w \times i_{corr} \times t}{F} \quad (5)$$

where:

$m$  Mass loss, g  
 $E_w$  Fe equivalent weight = 28 g  
 $t$  Time (year in s) = 31 536 000 s  
 $F$  Faraday constant = 96 500

Mass Loss:

$$m = \rho \times V \quad (6)$$

Volume:

$$V = A \times d \quad (7)$$

where:

$\rho$  Fe density = 7.86 g/cm<sup>3</sup>  
 $A$  Area exposed (input during measurement), cm<sup>2</sup>

$d$  Corrosion thinning = CR, mmpy  
 10 Conversion factor from cm to mm

So,

$$\rho \times A \times d = \frac{Ew \times icorr \times t \times 10}{F}$$

$$\rho \times A \times d = \frac{Ew \times t \times 10}{F} \left( \frac{\beta}{Rp} \right)$$

$$d = \frac{Ew \times t \times 10}{F \times \rho} \left( \frac{\beta}{Rp \times A} \right)$$

$$Cf = \frac{Ew \times t \times 10}{F \times \rho} \quad (8)$$

Note: When A (area) has been input in Cell Info to determine Rp, area is no considered in (9)

$$CR = Cf \frac{\beta}{Rp} \quad (9)$$

where:

$Cf$  Conversion factor determined as per Equation (9)  
 $CR$  Millimetres/year (mmpy) (9) [5]  
 $Cf$  11 641.66

### 3. Results & Discussions

#### 3.1 Overall Assessment of this Plant Trial During Acid Wash

The electrochemistry techniques used in this trial are genuine measurements of the instant corrosion behavior of the materials under the process line corrosion environment. Plant process conditions, such as suspended solids, increased ionic impurities as a result of desilication product (DSP) dissolution, do not have any impact on the data collection quality.

However, flow dynamics through the pipe, such as air pockets in the liquid flow, intermittent flow velocity due to pump problems, etc, have a significant impact on the quality of data (noisy signal), especially when measuring impedance. This problem was observed in the low-frequency range of the measuring device (potentiostat) which corresponds to the high X-axis value of the Nyquist plot as shown in Figure 7.

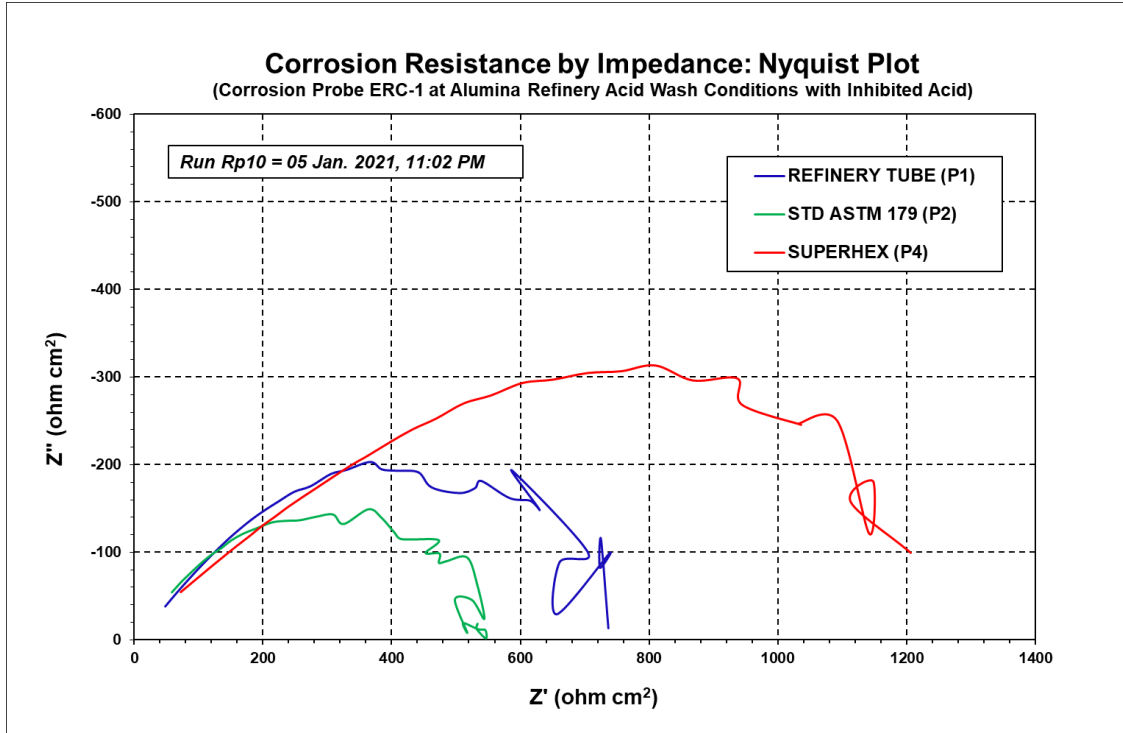


**Figure 7. Plant data of Run Rp10**

The plot showed in Figure 8, is a laboratory replication (same plant temperature) of plant Run Rp10 using the same acid brew from Tk 30 before injection, and a replicated corrosion probe. This replication falls within the plant measurement range and removes the noise from the affected area during the plant run. Most of the runs carried out during this acid wash show the Superhex with higher corrosion resistance under real plant acid wash conditions as shown in Figures 7 & 8.

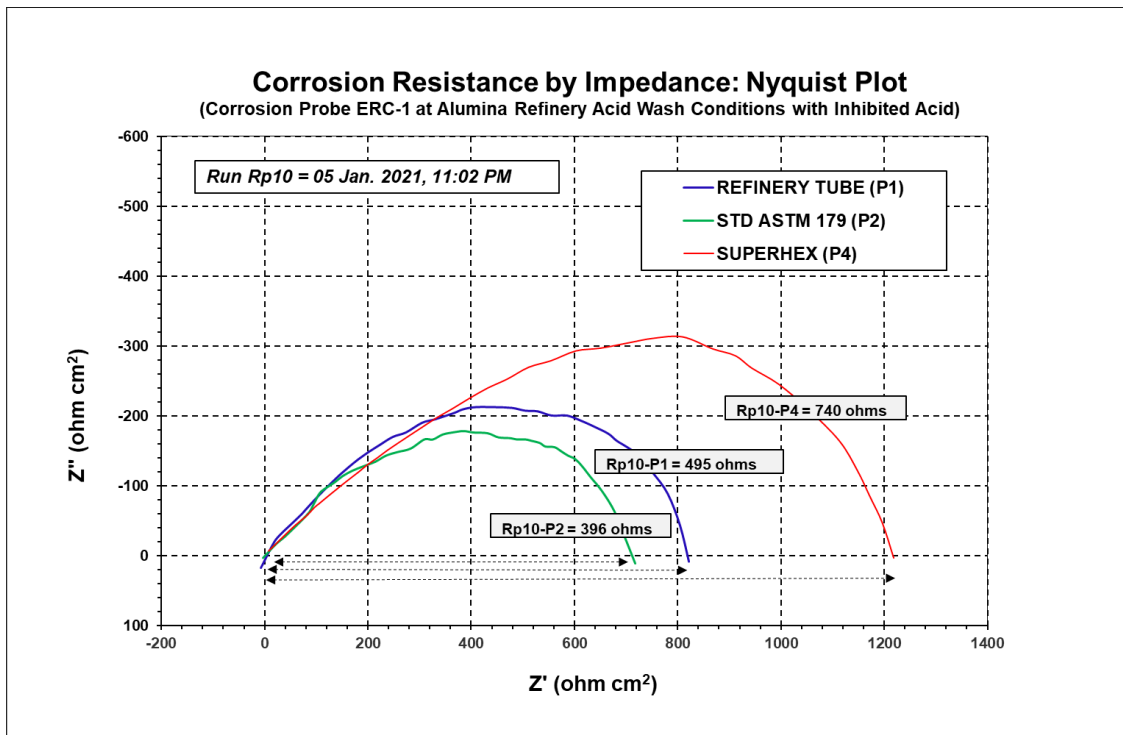


**Figure 8. Laboratory data of Run Rp10 during acid washing**

### 3.2 Overall Assessment of this Plant Trial During Liquor Flow

The data collection during liquor flow showed less noise consequently, did not need correction. The data shows typical corrosion resistances during normal operations at full steam temperature conditions. The Nyquist plot semicircle is not completed due to instrumentation set up however, the corrosion software can calculate corrosion resistance.

Most of the runs carried out during Bayer liquor show the Superhex with higher corrosion resistance as shown in Figure 9.

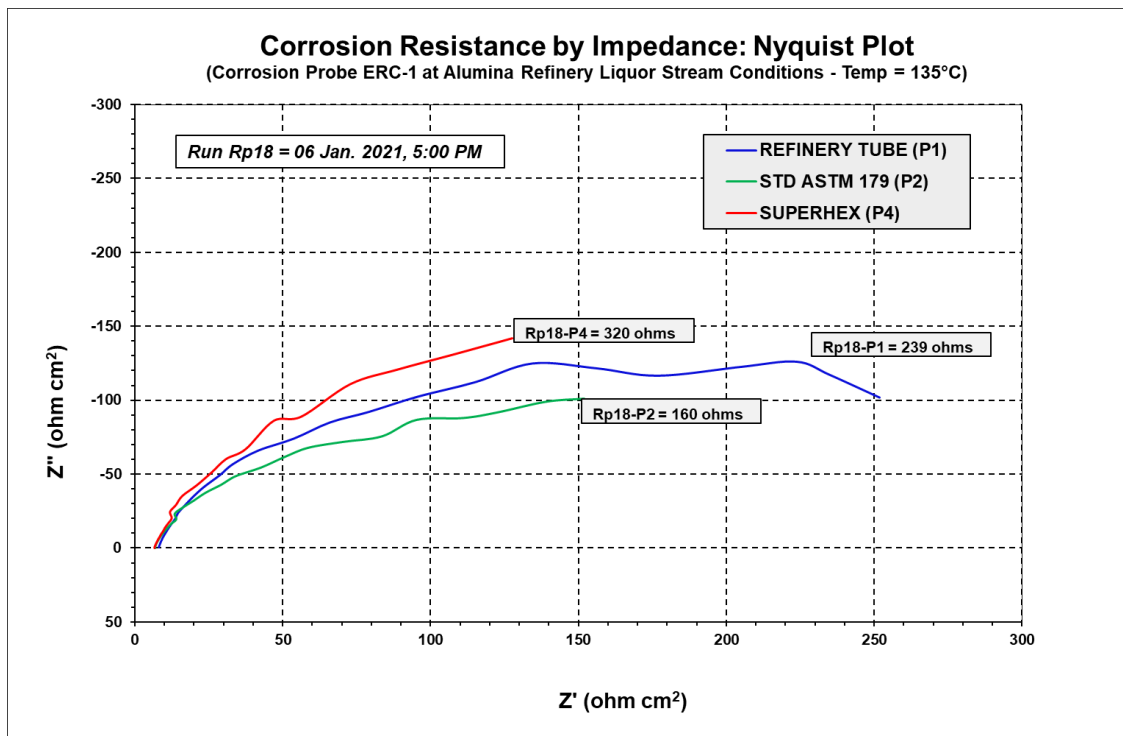


Figure 9. Plant data of Run Rp 18 during Bayer liquor flow

### 3.3 Corrosion Rate During Acid Wash

LPR data was used to calculate corrosion rate. Acid from TK 30 started been injected into the system on Tuesday the 05/01/2021 at about 21:00 hours and finished at about 23:30 hours. This longer than usual injection time was due to operational problems no clearly explained to the author. Acid recirculation started immediately after this, and finished on Wednesday the 06/01/2021 at about 02:00 hours.

The corrosion rates were kept between 0–5 MMPY along the injection and recirculation periods with pronounced spikes at the beginning of the injection period and less pronounced spikes afterwards as shown in Figure 10.

Results depicted in Figure 10, indicate satisfactory level of protection along the injection and recirculation stages. Corrosion rates values between 0–5 MMPY provide a well inhibited system for low carbon steel. High corrosion rate at the beginning of the acid injection may indicate the depleted level of inhibition of the first acid reaching the probe as a result of the consume on the whole metal surface prior to the probe. This is inhibitor consumed on the piping surface between Tank 30 and the probe. This is however, a short transition stage with minor impact on the overall integrity of the HEX tube. Under these conditions, all materials under evaluation show similar level of protection.

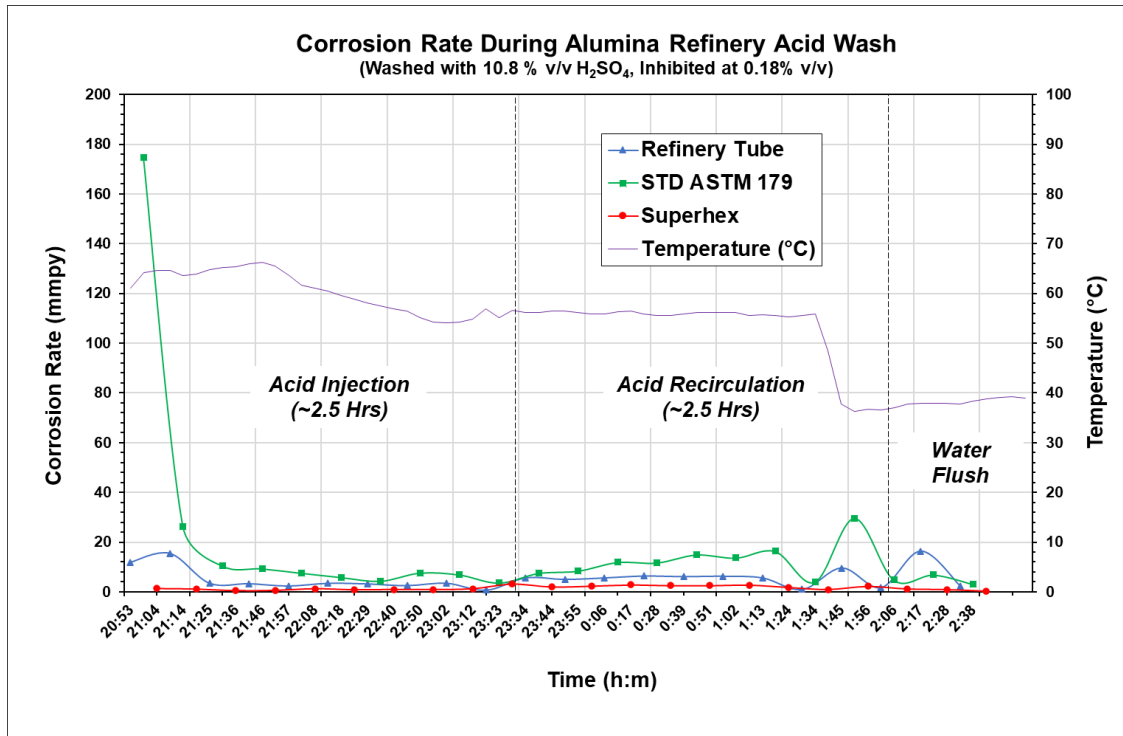


Figure 10. Corrosion rate during acid wash

### 3.4 Corrosion Rate During Bayer Liquor Flow

After a few intents to start the liquor pump, it finally started injecting Bayer liquor into the system on Wednesday the 06/01/2021 at about 13:22 hours starting at 75 °C. As the temperature increased, the corrosion rate tended to increase also reaching the highest value as steam was injected into the system. The corrosion rate levels were kept between 0 and 0.04 mmpy as shown in Figure 11.

Results depicted in Figure 11, during liquor flow, indicate a satisfactory level of protection. Added to the inherent passive nature of caustic solution in low carbon steel, the corrosion rates are between 0–0.04 mmpy.

Gradual increase of temperature during passivation and steam injection still brings the corrosion rate to acceptable levels. Under these conditions, the Superhex (red line) always showing the lowest and steadiest level of protection

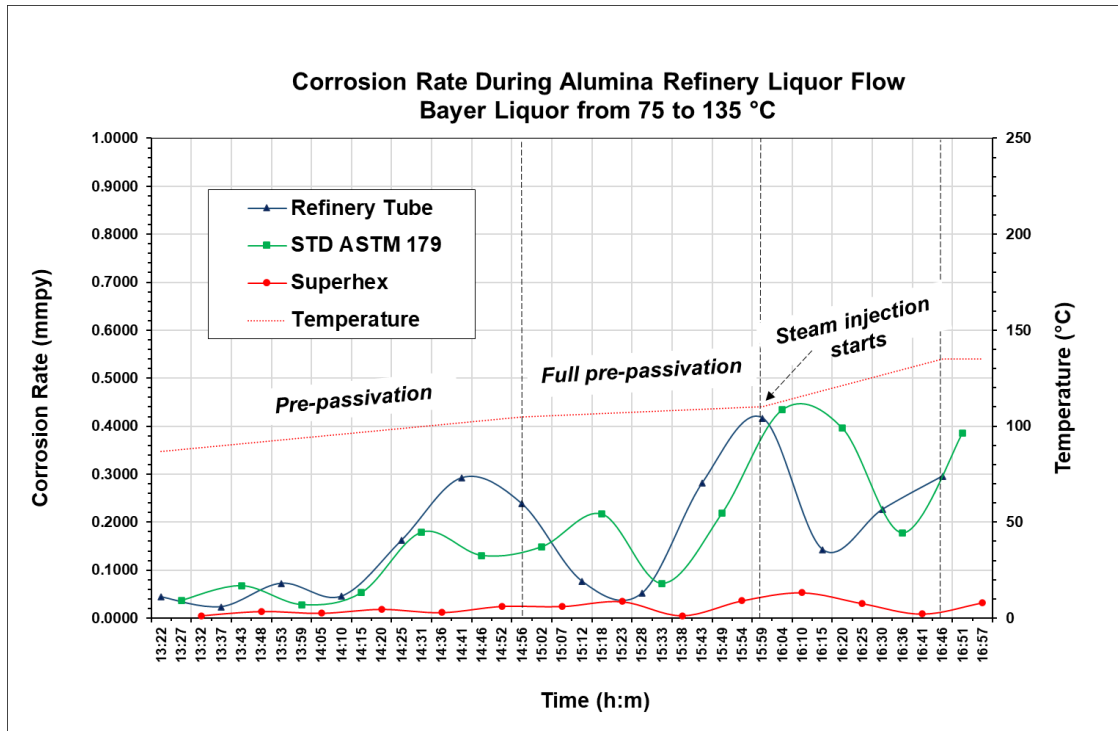


Figure 11. Corrosion rate during Bayer liquor flow

### 3.5 Dose-Response of Corrosion Inhibitor PIC 515

This is laboratory-generated data that depicts the degree of adsorption on the metal material as the dose of corrosion inhibitor is increased from no protection to fully protected condition. This test was performed at refinery acid cleaning conditions for temperature.

As seen in Figure 12, the three materials under evaluation have different levels of adsorption at the beginning of the trends and they tend to equal and reach full inhibition levels as the dose increases. It can also be observed that metal materials reach maximum protection (lower corrosion rate) at a certain dosage and beyond that, additional corrosion inhibitor does not provide any extra protection.

PIC 515 has been formulated as a dispersible but not fully soluble substance in aqueous solutions. Liquids of this nature, once reaching high concentrations, tend to come up to the top and concentrate at the water surface when there is no agitation.

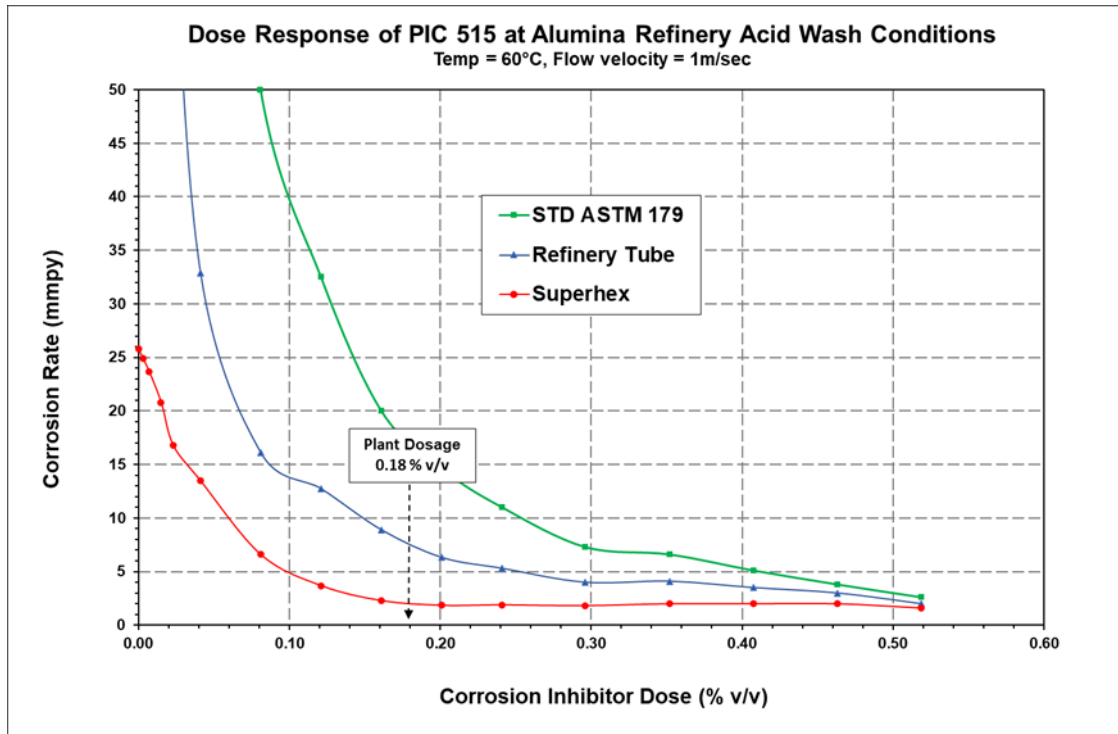


**Figure 12. Laboratory dose-response of corrosion inhibitor PIC 515**

The laboratory experimental work depicted in Figure 12 has reached a maximum dose of 0.5188 % v/v and did not show corrosion inhibitor concentrated on the water surface. This may indicate that the acid brew used on 05/01/2021 has more likely overdosed above 0.5188 % v/v. This could also explain the reason that during plant acid wash depicted in Figure 9, there is no discrimination between Superhex and the other two materials in terms of corrosion rates. The materials were just exposed to a well-overdosed acid brew.

### 3.6 Temperature Response of Corrosion Inhibitor PIC 515

This is also laboratory-generated data that shows how strong the corrosion inhibitor adsorption onto the metal surface is as the temperature increases. The test was done at a complete inhibition level, in this case, 0.18 % v/v, and then the temperature was gradually increased to a level where the corrosion rates compromised the integrity of the HEX tube.

As per trends depicted in Figure 13, the temperature has a great effect on corrosion rate and this is related to the chemical formulation of the corrosion inhibitor and the metallurgy of the metal surface.

In most of the cases using diluted sulphuric acid, the corrosion rate becomes exponential as the temperature increases.

Most of the more effective corrosion inhibitors used in acid solutions are organic base chemicals. Some organic chemicals break down the carbon chain under temperature and lose their property as effective corrosion inhibitors. The metallurgy of the metal surface with regards to microstructure and chemical composition is strongly related to the degree of adsorption.

As we see in Figure 13, Superhex performs better with the current corrosion inhibitor by providing strong adsorption up to 70 °C.

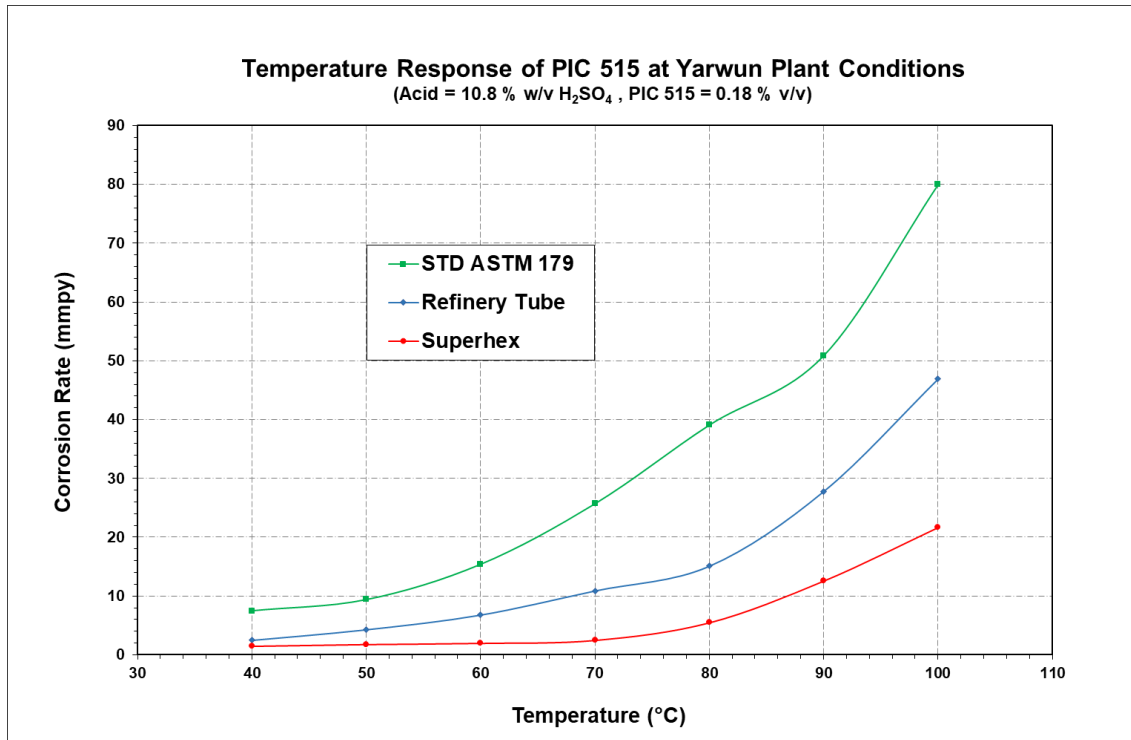


Figure 13. Laboratory temperature response of corrosion inhibitor PIC 515

#### 4. General Comments and Room for Improvement

Superhex will provide a solid backup to the current operational acid washing procedure due to its high corrosion resistance to uninhibited and inhibited diluted sulphuric acid and good surface adsorption to the current corrosion inhibitor PIC 515.

Corrosion inhibitors are key components to minimize corrosion damage to low carbon steel exposed to dilute sulphuric or hydrochloric acid. All alumina refineries use corrosion inhibitors to protect their HEX tube exposed during acid wash. The reality is, under this protected environment, the range of life span of their HEX tubes varies from 3 to 5 years (digestion heaters) which is considered low. The tube life span of the tube should be above 5 years. This indicates that the high level of protection given by the inhibitor at a particular time is not kept along with the operational life of the tube. Appears to be that the inhibitor protection has not always been there as it should be, as a result, various degrees of corrosion damages have always happened. A high corrosion resistance material based on its inner metallurgy, such as the Superhex, will always be there to mitigate corrosion attack and will enhance the protection with a suitable corrosion inhibitor and reaching life spans well beyond 5 years.

The data obtained on this plant trial and the related laboratory tests highlight the fact that there is room for improvement within the current system.

The following ballot points are for comment and discussion:

- Formulate a new corrosion inhibitor that is fully soluble in acid solution, with a faster dose-response to the Superhex surface and the existing HEX tube surface remaining in the evaporation trains.
- Optimize the acid wash exposure time to the metal surface based on the complete dissolution of the DSP scale.
- If required, modify the current location of the inhibitor injection point at the top of Tank 30 to make sure that the entire dose reaches the acid solution.

- Coordinate another visit to discuss the content of this report and perform another short data collection series to determine the exact process time required for the acid solution to dissolve the DSP scale deposited on the existing online corrosion probe ERC-1.

## 5. References

1. M.G. Fontana, *Corrosion engineering*, 3<sup>rd</sup> Edition, McGraw-Hill Book Company, 1985.
2. M.J. King, W.G. Davenport, M.S. Moats, *Materials of construction, sulfuric acid manufacture - analysis, control, and optimization*, 2<sup>nd</sup> Edition, Elsevier, San Diego, Calif, 2013, pp. 349-356.
3. S. Lyon, Overview of corrosion engineering, science and technology, *Nuclear Corrosion Science and Engineering*, Elsevier Ltd 2012, pp. 3-30.
4. F. Mansfeld, Tafel slopes and corrosion rates obtained in the pre-Tafel region of polarization curves, *Corrosion Science*, 47 (2005) 3178-3186.
5. ASTM G102-89(2015)e1, Standard practice for calculation of corrosion rates and related information from electrochemical measurements, *ASTM International*, West Conshohocken, PA, 2015.
6. ASTM G59-97(2014), Standard test method for conducting potentiodynamic polarization resistance measurements, *ASTM International*, West Conshohocken, PA, 2014.
7. C. Gabrielli, M. Keddam, H. Takenouti, *The use of a.c. techniques in the study of corrosion and passivity*, 23 (1983) 395-451.
8. J.P. Diard et al., Calculation, simulation and interpretation of electrochemical impedance. Part II. Interpretation of Volmer-Heyrovsky impedance diagrams, *Journal of Electroanalytical Chemistry and Interfacial Electrochemistry*, 255 (1988) 1-20.
9. F. Mansfeld, Analysis and interpretation of EIS data for metals and alloys, *Technical Report No. 26*, University of Southern California, Los Angeles, CA, USA, 1999.
10. H.P. Stüwe, A.F. Padilha, F. Siciliano, Competition between recovery and recrystallization, *Materials Science and Engineering: A*, 333 (2002) 361-367.